

Chapter 1

Holographic Visualization of Shock Wave Phenomena



1.1 Introduction

Gabor (1948), for the first time, presented the concept holography. In 1971, the Nobel Prize in physics was awarded on him for his invention of holography, which opened a new era in the flow visualization. This was a long time before the advent of the lasers. Encouraged by the development of lasers, Light beams are characterized by their amplitude and phase angle. Leith and Upatnieks (1962) developed off-axis holography in which object and reference beams, *OB* and *RB*, illuminate on a holographic film with an off-axial direction and became a basis of modern holographic interferometry.

Shadowgraph and schlieren methods are traditional ways for visualizing compressible flows. Their principle is based on recording, on film, amplitude variations induced by the density changes associated with the flows, whereas holography uniquely records changes in phase angles of light beams induced by changes in considered flows.

Wortberg (1974) and Russell et al. (1974), for the first time, reported the usefulness in visualizing shock tube flows and their results were reported wave at the 9th International Shock Tube Symposium held at Stanford University. Russell et al. (1974) visualized the flow developed in a Ludwig tube flow. The vortex formation from the trailing edge of a wing-section was visualized by Mandella and Bershader (1986).

In 1975, equipped with a ruby laser which was one of the first generation products in Japan, we struggled to apply it as light source for visualizing shock tube flows. In 1980, we eventually purchased a double pulse holographic ruby laser and started to intensively visualize shock tube flows and underwater shock waves by holographic interferometry. Its first outcome was for the first time reported in Takayama (1983).

1.2 Double Exposure Holographic Interferometry Applied to Shock Wave Research

A schematic diagram of holographic interferometric system applied to shock tube flows at the Shock Wave Research Center (SWRC) of the Institute of Fluid Science, Tohoku University is illustrated in Fig. 1.1, Takayama (1983). Light sources were Q-switched ruby lasers (Apollo Lasers Ltd. double pulse holographic ruby lasers, pulse width of 25 ns, 695.4 nm wavelength and 10 and 2 J/pulse at TEM_{00} mode and a single pulse ruby laser, pulse width of 25 ns, 695.4 nm wavelength and 2 J/pulse at TEM_{00} mode). The beam was divided, by using a beam splitter *BS*, the 60% of the source laser beam was directed into object beam *OB* and 40% into reference *RB*.

The optical path of the *OB* is identical to the observation beam of the conventional optical arrangements, while the *RB* is unique to holographic interferometric arrangement, takes the identical light path length as the *OB* and independent of the events preserves the phase angle of the light source. Then when the *OB* and *RB* are superimposed on holographic films, we can identify the variation of phase angles caused by the event.

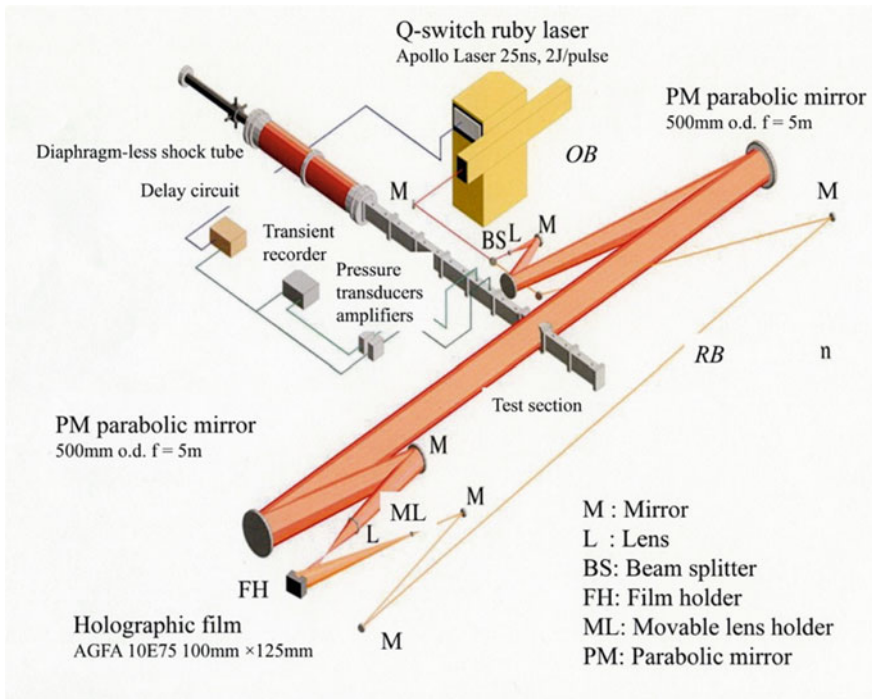


Fig. 1.1 An optical arrangement of holographic interferometry applied to shock tube research at the Shock Wave Research Center of the Institute of Fluid Science, Tohoku University

In order to collimate OB , we used paraboloidal schlieren mirrors of 300 mm diameter and 3000 mm focal length and 500 mm diameter and 5000 mm focal length. The surface finish of the used mirrors was a quarter to one tenth of the light wavelength. In order to visualize larger fields of view, a pair of paraboloidal mirrors having 1000 mm dia. and 8000 mm focal length was introduced. The single mirror and its steel base weighing about 300 kg, we mounted them on a steel box the bottom of which had 1.5 mm diameter holes evenly distributed. We can make the box and the mirror move freely and align precisely.

The source laser beam is collimated with a plano-concave lens of short focal length to a slightly larger diameter OB and only the central part of the source light passes the test section.

The difference of path lengths between OB and RB is adjusted to be less than the coherent length of the source laser. The OB and RB illuminated simultaneously a holographic film @laced on a film holder, FH, at the approximately 20° . In order to satisfy the condition for linear transmittance of holographic recording materials the ratio of OB and RB intensities ranges between 2:1 and 3:1. Holographic films, AGFA 10E75 100 mm \times 125 mm sheet films, was placed on a film holder FH made of thick aluminum plate and coated black, on the surface of which 2 mm dia. holes were uniformly distributed. Films were held flat, when slightly reduced pressures were applied through the perforation Takayama (1983).

In general, when a hologram was illuminated by a coherent beam, the reconstructed images are three-dimensional virtual ones. Although reconstructed images are three-dimensional and can be readily recognized with naked eyes but are hardly recorded on films. The three-dimensional images were recorded from various view angles. Although, as shown later, spatial resolution of the reconstructed images is not as sharp as that of the holograms' image, the resolution would be improved if properly processed by a computer assisted image processing systems.

In the double exposure holographic interferometry, the first exposure is performed prior to an event and the second exposure is synchronized with the event. Thus the change in phase angles during the double exposure was stored on a holo-film. Hence the time-interval of the double exposures should be short, which was automatically controlled by the source laser systems. We, however, often performed double exposures manually for time interval of several seconds. In such cases, the test conditions must be kept exactly unchanged throughout the double exposure. The phase change thus stored on the film can be reconstructed later through the process, the so-called process, reconstruction.

In flow visualizations by using double exposure holographic interferometry, the change in phase angles is uniquely expressed by the variations in the refractive indices. Hence, holographic interferometry is a method, unlike the Mach Zehnder interferometry, to quantitatively measure density fields with minimum restrictions on the optical arrangement. In double exposure holographic interferometry, inhomogeneity inherited from optical components, such as test section windows, media under study, may perturb the contrast of the background but will hardly distort fringe distributions. Hence, double exposure holographic interferometry is useful in visualizing shock waves in slightly inhomogeneous media such as liquids,

apparently transparent media, such as commercial glass plates and acrylic plates, and even in water and air exposed to a convection.

Fringes obtained in identical arrangement during the double exposures are named infinite fringes. In two-dimensional cases such as shock tube flows, the fringes are expressed with infinite width and correspond to equal-density contours. This is named infinite fringe interferometry.

When shifting and rotate the center of RB on FH in Fig. 1.1 either at the first or the second exposure and keeping OB unchanged, equal interval parallel fringes appear in reconstructed images. The orientation and the interval of fringes are determined by the degree of rotation and deviation from the initial state. In the holographic arrangement, RB was collimated with a 150 mm o.d. convex lens and superimposed with OB on FH . Figure 1.2a shows the 150 mm diameter lens, movable lens ML as illustrated in Fig. 1.1, mounted on a stage. As illustrated in Fig. 1.2b, the lens is rotated by θ and is swung by ε at either the first or second exposures. When adjusting ε and θ , the interval and orientation of fringes are arbitrarily selected. Changes of phase angles during the double exposures are expressed by the deviation of fringes from their regular intervals. This is named as a finite fringe interferogram. It was not easy to measure the deformation of fringe distributions. However, today, the deviation of fringe distribution from its initial position are relatively easily determined by using a computer-assisted image processing system (Houwing 2005).

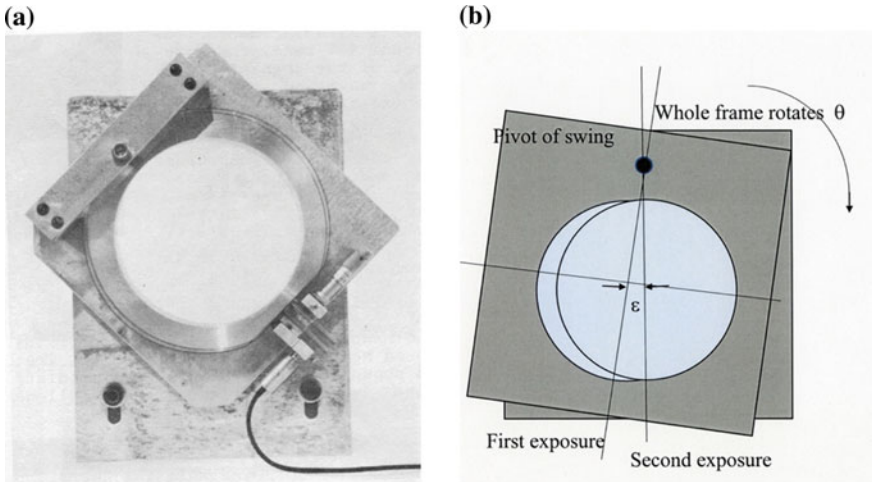


Fig. 1.2 Movable lens mount: **a** a movable lens mount; **b** an illustration of movable mount Takayama (1983)

1.3 Analytical Background of Holographic Interferometry

To apply holographic interferometry to shock tube experiments, the light source should be a Q-switched laser having a high coherency. In 1980, Q-switched ruby lasers having a pulse duration of 25 ns and wavelength of 694.3 nm were used. The source laser beam is split into object beam *OB* and reference beam *RB*, to be called U_{ob} and U_{re} , respectively. Let subscripts 1 and 2 refer to the first and second exposures, respectively. ω is the frequency of the ruby laser, where the light speed $c = 2\pi\omega\lambda$ and λ is the wave length of 694.3 nm. Hence *OB* and *RB* in the first and second exposures are expressed as

$$U_{k,ob}(x, y) = a_{k,ob}(x, y) \exp\{i\omega t + i\phi_{k,ob}(x, y)\},$$

where $k = 1$ for first exposure and 2 for second exposure,

$$U_{k,re}(x, y) = a_{k,re}(x, y) \exp\{i\omega t + i\phi_{k,re}(x, y)\} \quad (1.1)$$

where $a_{k,ob}(x, y)$ and $a_{k,re}(x, y)$ are the amplitude distributions of the *OB* and *RB* for the first and second exposure and $\phi_{k,ob}(x, y)$ and $\phi_{k,re}(x, y)$ are their phase distributions, respectively.

The amplitude I_1 of light waves recorded on the holofilm at the first exposure is expressed as $U_{1ob} + U_{1re}$.

$$\begin{aligned} I_1 &= |U_{1ob} + U_{1re}|^2 \\ &= (U_{1ob} + U_{1re})(\underline{U_{1ob} + U_{1re}}), \end{aligned} \quad (1.2)$$

where $\underline{U_{1ob} + U_{1re}}$ is complex conjugate of $U_{1ob} + U_{1re}$.

In the second exposure, the *OB* which is represented as $U_{2ob}(x, y)$ carries not only the amplitude variation but also the phase variation, whereas $a_{re}(x, y)$ and $\phi_{re}(x, y)$ are spatially uniform and constant.

In constructing finite fringe interferograms, we inserted a collimating lens in the cutoff side of the *RB* path and displaced its center during the double exposures. By displacing the collimating lens and rotating the angle of the axis of the collimating lens, we controlled the phase angle $\Delta\phi$ between the first and second exposures. The interval and orientation of finite fringes were readily adjusted.

In constructing infinite fringe interferograms, we fix the collimating lens unchanged during the double exposure, which means having identical $\Delta\phi$ during the first and second exposures. Then the fringe interval becomes infinitely wide. Hence, infinite fringe interferometry was achieved.

The total intensity of illuminating light beams on the film which transmits only the amplitude of the light is given;

$$I(x, y) = (U_{1ob} + U_{1re})(\underline{U_{1ob} + U_{1re}})(U_{2ob} + U_{2re})(\underline{U_{2ob} + U_{2re}}) \quad (1.3)$$

Although the relationship between the recorded light intensity $I(x, y)$ and the transmittance of the film Ta is, in general, nonlinear, for some types of recording materials and light intensity, if the ratio of OB to RB is sufficiently large, a linear relationship is valid between Ta and $I(x, y)$ (Gabor 1949). In order to achieve this condition, the ratio of OB to RB is, in practice, empirically chosen to be approximately 2:1–3:1. Therefore, the amplitude transmittance of the film Ta is given by, $Ta = k_0 + k_1 I(x, y)$ where k_0 and k_1 are constant.

If a hologram is illuminated with RB , $U_{re} = a_{re} \exp(i\omega t + i\phi_{re})$, the wave field emerging on the hologram with an amplitude transmittance Ta , is

$$TaU_{re} = \{k_0 + k_1 I(x, y)\}U_{re}.$$

The amplitude distribution $T(x, y)$ of the reconstructed image has a physically meaningful term, which can be rewritten as,

$$T_3 = k_1 a_{re}^2 a_{2ob} \exp(i\phi_{1ob} + i\omega t) + \exp(i\phi_{2ob} + i\omega t) \quad (1.4)$$

This term represents the reconstructed phase change recorded during the double exposures. The relationship between phase changes and the fringe intensities of the reconstructed double exposure holographic interferogram is derived from Eq. (1.4) to read,

$$I_{reconstruct} = T_3^2 = (k_1 a_{re})^2 a_{ob}^2 \{1 + \cos(\phi_1 - \phi_2)\} \quad (1.5)$$

Equation (1.5) means that the fringes this reconstructed in interferograms correspond to the difference in the phase angle during the double exposures. In case $\phi_1 - \phi_2 = 2\pi N$, where the fringe number N is integer, $I_{reconstruct}$ is a maximum showing dark interference fringes. As changes in phase angles indicate the variations in the refractive indices along the light path; when the flow is two-dimensional flow, the fringe distribution just correspond to the variation of refractive indices. The following relationship is valid,

$$\phi_1 - \phi_2 = 2\pi L(n_1 - n_2)/\lambda, \quad (1.6)$$

where L and λ are the light path length and the light wave length. $n_1 - n_2$ stands for changes in refractive indices.

In gases, the refractive index n is related to the density ρ as follows.

$$n - 1 = K\rho, \quad (1.7)$$

where K is the Gladstone-Dale constant, which varies with λ . So far as the experiments are performed by using ruby laser, K is constant.

In liquids, the refractive index and density is related via Lawrence-Lawrentz relations

$$(n^2 - 1)/(n^2 + 2) = C\rho, \tag{1.8}$$

where C is constant. In gases, the refractive index n is written as $n = 1 + \epsilon$ and $\epsilon \ll 1$, and hence Eq. (1.8) reduces to Eq. (1.9).

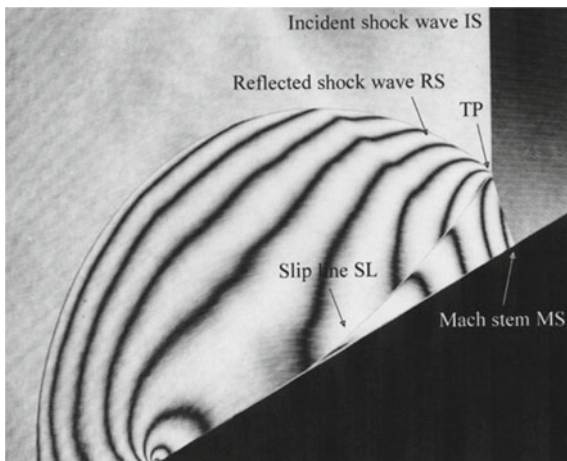
$$\Delta\rho = N\lambda/KL \tag{1.9}$$

We can readily determine the density distribution by counting dark fringes which correspond to phase angle of $2 N\pi$. By counting dark fringes, we can readily identify the density distribution. Brightest fringes correspond to the phase $(2 N + 1) \pi$. Likewise, by measuring the grey level of fringes between neighboring dark and bright fringes, enable one to correctly estimate the phase angle of corresponding grey level and hence to interpolate density between dark and bright fringes.

Figure 1.3 demonstrates, for example, an infinite fringe interferogram of a shock wave of $M_s = 1.50$ in air reflected from a 25° wedge. The back fringes correspond to equal density contours indicating phase angle of $2 N\pi$ likewise the white fringes correspond to phase angle of $(2 N + 1) \pi$. Knowing fringe numbers, the density contours are readily determined.

The eight-digit number allocated to this interferogram shows a ID number, for example, #92090404 indicates that this interferogram was taken in 1997, 4th of September and the results of No. 4th experiment.

Fig. 1.3 #92090404, single Mach reflection SMR over a 25° wedge for $M_s = 1.50$ in air in $60 \text{ mm} \times 150 \text{ mm}$ shock tube



References

- Gabor, D. (1948). A new microscopic principle. *Nature*, *161*, 777–778.
- Gabor, D. (1949). Microscopy by reconstructed wave fronts. *Proceedings of the Royal Society of London*, *197*, 454–487.
- Houwing, A. F. P., Takayama, K., Jiang, Z., Sun, M., Yada, K., & Mitobe, H. (2005). Interferometric measurement of density in nonstationary shock wave reflection flow and comparison with CFD. *Shock Waves*, *14*, 11–19.
- Leith, E. N., & Upatnieks, J. (1962). Reconstructed wave fronts and communication theory. *Journal of the Optical Society of America A*, *52*, 1123–1130.
- Mandella, M., & Bershader, D. (1986) Quantitative study of shock-generated compressible vortex flows. In D. Bershader & R. Hanson (Eds.), *Proceeding 15th International Symposium on Shock Waves and Shock Tubes Shock Waves and Shock Tubes* (pp. 471–477) Berkeley.
- Russell, D. A., Buonadonna, V. R., Jones, T. G. (1974). Double expansion nozzle for shock tunnel and Ludwig Tube. In D. Bershader & W. Griffith (Eds.), *Recent developments in shock tube research*. In *Proceeding of 9th International Shock Tube Symposium* (pp. 238–249). Stanford.
- Takayama, K. (1983). Application of holographic interferometry to shock wave research. In *Proceeding SPIE 298 International Symposium of Industrial Application of Holographic Interferometry* (pp. 174–181).
- Wortberg, G. (1974). A holographic interferometer for gas dynamic measurement. In D. Bershader & W. Griffith (Eds.), *Proceedings of the International Symposium on Shock Waves Recent Developments in Shock Tube Research* (pp. 267–276) Stanford.